The enhanced Raman scattering of phonons in CaF_2 and MgO samples containing Ca and Li colloids

1994 J. Phys.: Condens. Matter 6 9647

(http://iopscience.iop.org/0953-8984/6/45/014)

J. Phys.: Condens. Matter 6 (1994) 9647–9657. Printed in the UK

The enhanced Raman scattering of phonons in CaF_2 and MgO samples containing Ca and Li colloids

M L Sanjuán, P B Oliete and V M Orera

Instituto de Ciencia de Materiales de Aragón, CSIC–Universidad de Zaragoza, Plaza San Francisco s/n, 50009 Zaragoza, Spain

Received 23 February 1994, in final form 23 June 1994

Abstract. We present Raman scattering spectra of CaF_2 samples containing Ca colloids and of MgO:Li with Li precipitates. The samples have been prepared by different thermal and irradiation treatments in order to achieve a range of colloid radii and density. The sizes of the colloids are determined by their optical absorption bands. Exciting in the surface-plasmon band of the metal colloid we observe surface-enhanced Raman scattering (SERS) of the whole density of states of CaF_2 or MgO phonons. The spectra are polarized and show a partial T_{2g} character for CaF_2. The intensity is enhanced as the laser energy approaches the colloid band maximum, where surface plasmons are excited. Comparing the results of different samples we find that the spectrum intensity is roughly proportional to the total amount of colloid material in the sample.

In order to explain the appearance of the one-phonon density of states and its resonant behaviour we discuss the validity of the classical electromagnetic model and propose a mechanism consisting of surface-plasmon excitation followed by electron transfer from the metal to the host and de-excitation in the metal–host interface. In the host, electron–phonon interaction takes place, as in usual Stokes or antiStokes processes, giving rise to single-phonon modes. The lattice distortion and loss of periodicity in the vicinity of the colloid break the $k = 0$ selection rule and account for the appearance of the whole density of states.

1. Introduction

In the 20 years since its discovery [1], the surface-enhanced Raman scattering (SERS) has been the subject of a great number of works both in the theoretical and experimental aspects. In spite of this effort, as stated in the recent review by Otto *et al* [2], 'a full understanding of all aspects of the enhancement mechanisms...is still missing'. One of the main points of discussion is whether the enhancement is of classical electromagnetic (EM) origin (long range) or 'chemical' (short range). We shall not repeat here the arguments for each of these models, which are comprehensively described, together with a compilation of previous work, in [2] and [3].

Most of the experimental work in SERS has focused on the enhancement of Raman activity of organic molecules close to or adsorbed on a metallic surface, usually Ag. Raman enhancement of the phonon density of states in crystals containing metallic colloids has also been reported. As far as we know, all the work in crystals refers to alkali halides containing Ag or alkali-metal particles [4–6].

In this article we report on the Raman enhancement of CaF_2 phonons due to the presence of Ca colloids. The advantage of CaF_2 with respect to alkali halides is that it has an allowed mode, which gives a good probe of the degree of activation of the other phonon modes and can help to elucidate the possible mechanism of enhancement. Our spectra are partially polarized, this depending on the plane on which scattering is performed. We find, as in

0953-8984/94/459647+11$19.50

previous work, a strong enhancement as the laser approaches the surface-plasmon (SP) excitation band (we shall sometimes call this the colloid band).

We also report on the observation of the MgO single-phonon density of states by SERS in Li colloids. In contrast, no enhancement of the Raman intensity was detected in MgO:Ni containing Ni colloids.

2. Experimental details

Raman spectra were measured in a Dilor XY spectrometer with an intensified diode-array detector. A Coherent Innova 200 Ar laser was used in the region 2.35–2.7 eV. The laser beam is focused onto the sample through a 50X objective. The laser power was typically 10–20 mW on the sample. We used pure CaF_2 or BaFCl as intensity standards in resonance experiments in order to correct for instrumental efficiency and slight laser misalignments. Back-scattering geometry was used in all cases. Measurements in the 2–2.1 eV range were performed using dye-laser excitation.

Metallic Ca particles in CaF_2 were produced using either additive-colouration (AC) or irradiation techniques. AC was performed following the method described in [7]. After colouration the samples presented the typical absorption spectrum of F and M (F pairs) centres. Thermal annealing of the AC specimens at temperatures between 200 and 300 °C produces the colloid absorption band, whose position and integrated area are related to the mean particle size and metal volume fraction, respectively [8]. Cation colloids are also produced by radiolysis at temperatures at which both anion vacancies and halogen interstitials are mobile. For CaF_2 this temperature is about 50 °C [9].

Table 1. r, mean colloid radius. N_p, number of metallic particles per unit volume. V_c, fractional colloid volume. I_R, relative intensity of the activated spectrum, in arbitrary units ($\lambda = 528.7$ nm, band 'E', $E_i \parallel E_s$). S_c, colloid surface per unit volume.

Sample	r (nm)	N_p ($cm^{-3} \times 10^{12}$)	$V_c(\times 10^{-6})$	I_R	S_c (cm^{-1})
S0	12	0.35	2.7	5	3.5
S1	3.5	20	3.6	8	16
S2	11	1.45	8.1	17.5	12
S3	25	0.25	17	31	11

Following these procedures we have prepared several samples with colloids of different sizes whose characteristics are given in table 1, as derived from the optical absorption bands shown in figure 1 for samples S1–S3. Sample S4 had been electron irradiated at very high doses (> 1 Trad) and presented such a high defect concentration that the absorption spectrum could not be measured. Sample S0 has been included in the table but not in figures 1 and 2, for simplicity. All samples show the α band at $\sim$ 380 nm due to F-type centres and a broad band around 550 nm due to Ca precipitates. Sample S3 presents also some shoulders at the low-energy side of the colloid band, due to F aggregates, and a narrow band at 470 nm of unknown origin, which, however, does not interfere with our experiments.

We have also studied samples of MgO doped with Ni and Li where metallic colloids of the impurity cation were produced by thermochemical reduction (courtesy of Dr Y Chen, Oak Ridge National Laboratory, USA). These samples presented very broad optical absorption bands with maximum near 550 and 580 nm, respectively. No F centres were detected in the MgO samples.

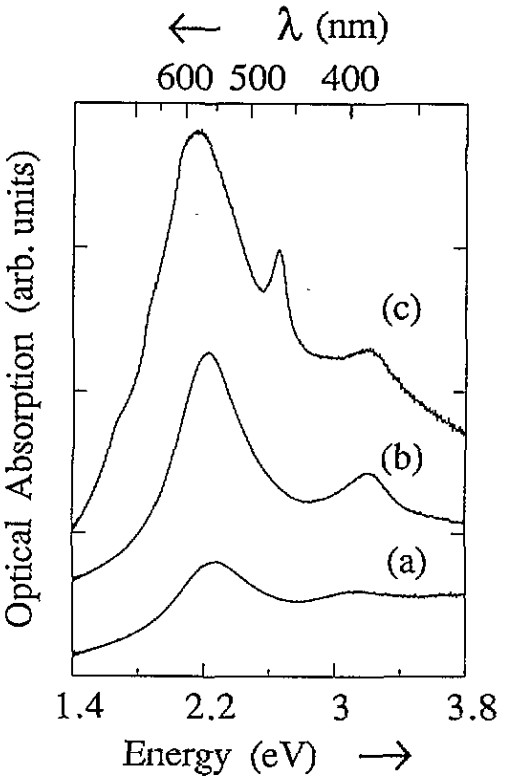

Figure 1. The optical absorption of samples S1 (curve a), S2 (curve b) and S3 (curve c). An offset has been added to spectra b and c for presentation purposes.

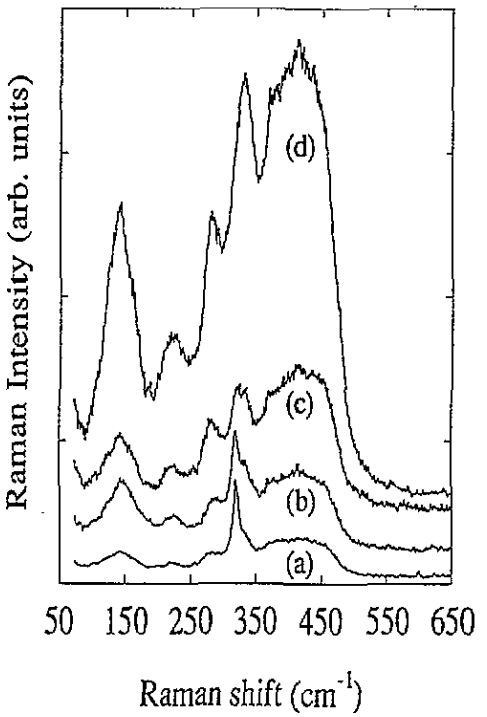

Figure 2. Raman spectra of S1 (curve a), S2 (curve b), S3 (curve c) and S4 (curve d) taken with $\lambda = 528.7$ nm (2.345 eV) and $E_i \parallel E_s$ on (111) faces for spectra a, c and d and (100) for b.

3. Experimental results

In figure 2 we present the Raman spectra of the four CaF_2 samples described in the previous section taken with $\lambda = 528.7$ nm and parallel incident and scattered electric fields ($E_i \parallel E_s$). Spectra of samples S1, S3 and S4 are performed in an arbitrary direction on a (111) face, while that of S2 is taken on a (100) face with electric fields along [110] directions.

Since CaF_2 has a unique Raman-allowed mode ($\nu_0 = 322$ cm^{-1}) seen as a strong, narrow peak in the spectrum of S1 and S2 (figure 2 curves a and b), all the accompanying structure is attributed to forbidden vibrations of the CaF_2 host activated by the presence of cation colloids. Though the main features are common to the spectra of all four samples, the whole intensity as well as the ratio between the allowed and forbidden spectra are greatly sample dependent, according to the amount and position of the colloid band. The activated spectrum is so intense in the S3 and S4 samples that the allowed mode is hardly seen. We found a roughly linear correlation between the intensity of the forbidden spectrum and the colloid volume fraction (see table 1). We will discuss in the final section of this paper the possible mechanisms originating such an activation.

In figure 3 we present the 514.5 nm spectrum of the S2 sample, on which we shall focus, with the scattered field E_s either parallel or perpendicular to the incident field ($E_i \parallel [110]$). Some peaks have been labelled for future discussion and data presentation.

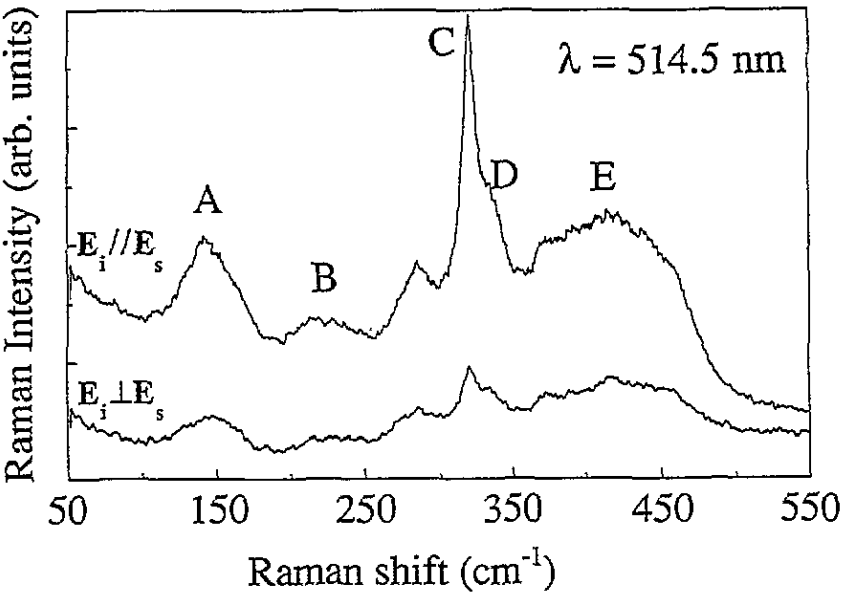

Figure 3. The Raman spectrum of S2 taken with $\lambda = 514.5$ nm (2.41 eV) in parallel and crossed polarizations with $E_i \parallel [110]$.

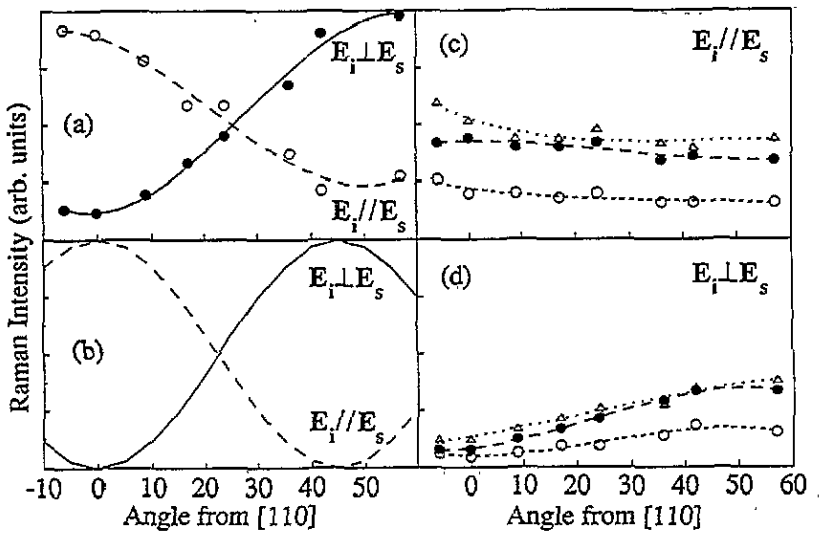

Figure 4. The angle dependence on a (100) face of Raman intensity for some phonon peaks as labelled in figure 3. $\theta = 0$ corresponds to the [110] direction. (a) The allowed mode; (b) the theoretical dependence for a T_{2g} mode. (c) Peaks A (●), B (○), E (△) in parallel polarization. (d) The same as (c) but crossed polarization. Experimental data are represented on the same vertical scale.

Figure 4 shows the angular evolution of the allowed- and forbidden-mode intensity as the angle θ between E_i and the [110] direction on the (100) plane is varied. We also give the variation expected for an allowed T_{2g} mode in O_h symmetry, corresponding to the ν_0 mode

of CaF_2. A remarkable difference is noticed between the evolution of the allowed mode and that of the rest of the spectrum. While the allowed-peak dependence is quite in agreement with the expected evolution, the forbidden spectrum shows little angular dependence when taken with $E_i \parallel E_s$ and a typical T_{2g} behaviour when $E_i \perp E_s$. This indicates that the activated spectrum does not have pure T_{2g} character: when measuring with $E_i \perp E_s$ we are selecting the T_{2g} contribution. On the other hand, all A_{1g}, E_g and T_{2g} vibrations can be seen in the parallel spectrum. The first two will add a constant level to the T_{2g} dependence shown in figure 4(b), which can result in an angular variation such as that of figure 4(c). Of course, since these modes are forbidden, they will probably not have a definite symmetry. Their polarization properties rather show that their character is mixed. The fact that the allowed-mode intensity does not fall to zero for $\theta = 0$ and $E_i \perp E_s$ (or for $\theta = 45°$ and $E_i \parallel E_s$) also means that it has partially lost its T_{2g} properties and contains some amount of forbidden character. We also recorded spectra of a (111) sample at different orientations. While for the allowed mode we found the $1:\frac{2}{3}$ ratio typical of a T_{2g} mode in this plane, the forbidden spectrum was more intense in parallel configuration, thus in agreement with the results of S2.

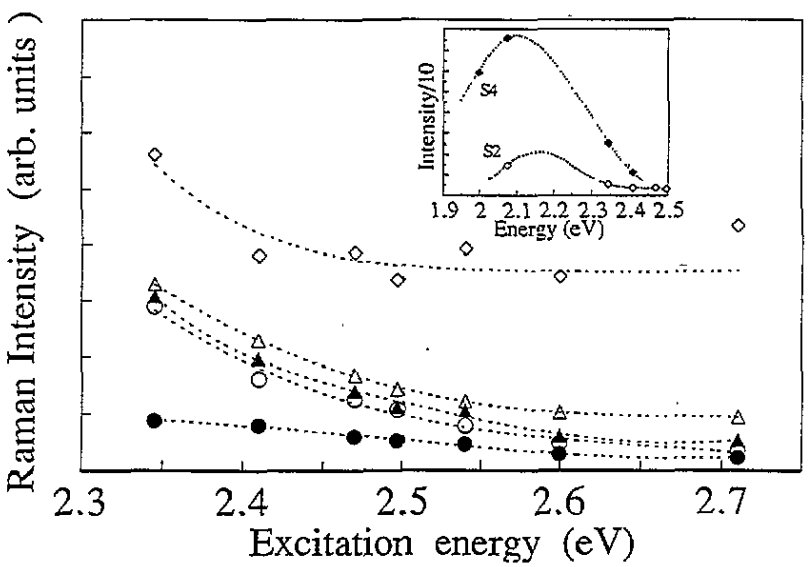

Figure 5. The excitation curves of peaks A (○), B (●), C (◇), D (▲) and E (△) with $E_i \parallel E_s$.

In figure 5 we present for sample S2 the Raman intensity against excitation energy of peaks labelled in figure 3. A clear resonant behaviour towards the longer wavelengths is seen for all the modes, except perhaps for peak B ($\nu \simeq 220$). Since this sample has the maximum of the colloidal band near 550 nm (2.25 eV) we ascribe the intensity enhancement to a resonance phenomenon within the colloid band. This is corroborated by the measurements performed in sample S4 at energies below the colloid band maximum (see the inset in figure 5). Due to the low detector sensitivity in this energy range as well as the low excitation powers achieved with the dye laser, the only sample that provided a good spectrum quality was the most doped one, S4. The fact that the allowed mode shows a weaker resonant enhancement is in agreement with this interpretation: part of it is due to regions of CaF_2 not perturbed by the colloids; only that part of the peak arising from

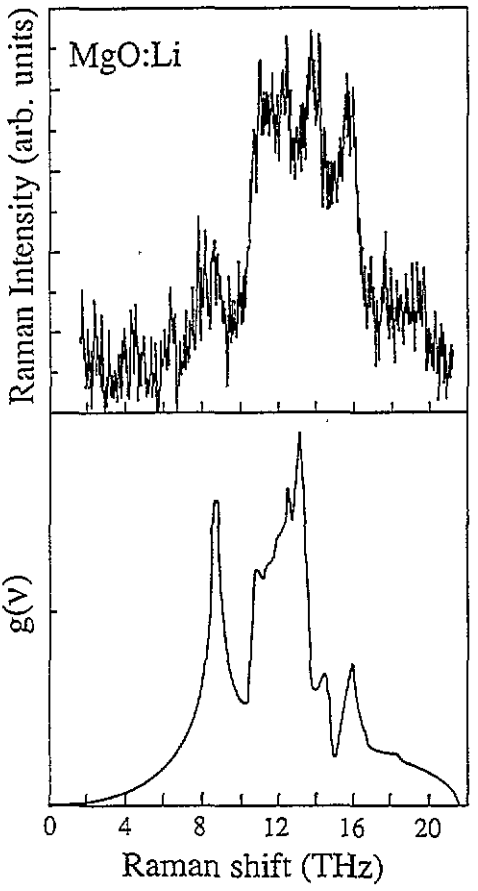

Figure 6. Top, the Raman spectrum taken with $\lambda =$ 514.5 nm of an MgO:Li sample containing Li colloids. Bottom, the phonon density of states of MgO (from [12]).

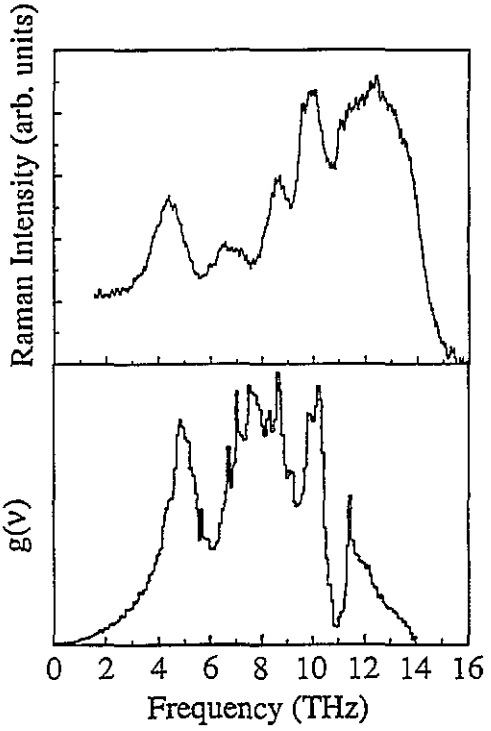

Figure 7. Top, the Raman spectrum of S2 with $\lambda =$ 514.5 nm and $E_i \parallel E_s \parallel [100]$. The allowed mode is not seen in this configuration. Bottom, the phonon density of states of CaF_2 (from [13]).

regions close to the metallic particles will resonate in the SP band. This point is further discussed at the end of the paper.

We have also performed Raman experiments in MgO crystals with metallic colloids. In MgO:Ni containing Ni colloids, where the broad colloid band is well within the range of the Ar laser [10], the phonon density of states is not observed. In contrast, it is found in MgO:Li with Li colloids having a band maximum between 550 and 600 nm [11]. We give in figure 6 the Raman spectrum of MgO:Li and the phonon density of states of MgO [12].

4. *Discussion*

The forbidden spectrum is interpreted as due to first-order vibrations of CaF_2 activated by the presence of colloids. Other possibilities are readily discarded: double phonons would extend up to much higher frequencies; local modes around vacancies or defects would not account for the high intensity observed nor for its resonant behaviour when the laser approaches the maximum of the colloid band. In figure 7 we compare the Stokes spectrum of S2 taken

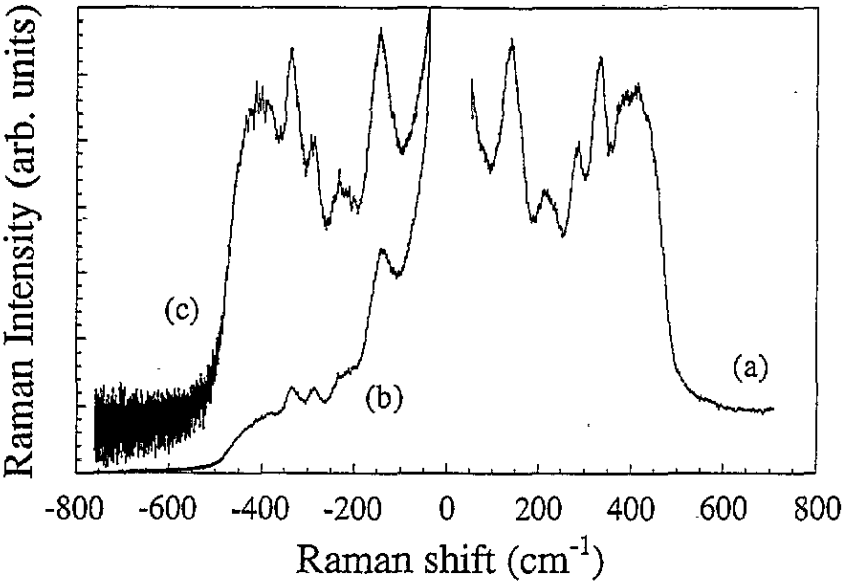

Figure 8. Stokes (curve a) and antiStokes (curve b) spectra of sample S4 taken with $\lambda = 514.5$ nm. Spectrum c is the same as b but multiplied by $(n + 1)/n$ so as to compare with a.

with $E_i \parallel E_s \parallel [100]$, where the allowed mode has a minimum, with a one-phonon density of states of CaF_2 [13]. The spectrum has been divided by the Bose factor $(n + 1)$ after a constant background was subtracted. Other frequency-dependent factors appearing in the Raman scattering cross-section [14] have not been taken into account since their dependence is unknown. Though there is a clear discrepancy in the relative intensities, mainly in the 10–14 THz region, the positions of the main features, associated with the critical points of the phonon density of states, are reproduced in the experimental spectrum. Considering that the coupling of different vibrations may be of different strength, the agreement is still remarkable. The fact that the major discrepancy occurs in the region of LO phonons indicates that their electron–phonon coupling is much stronger than for the rest of the phonons. The same feature is found for MgO (figure 6). We looked for 'hot-phonon' non-equilibrium by measuring the Stokes/antiStokes ratio, as shown in figure 8 for sample S4. Curves a and b correspond to Stokes and antiStokes spectra, respectively, and curve c shows the antiStokes spectrum multiplied by the $(n+1)/n$ quotient, where n is the Bose factor and $kT = 300$ K. The almost perfect coincidence between a and c clearly means that thermal equilibrium has been established (with negligible heating) and no anomalous phonon population is detected. The constant background observed in the Stokes side beyond 500 cm^{-1} is probably due to the electronic continuum arising from intracolloid transitions, similar to those observed in alkali halides containing Ag particles [5, 6].

Now we discuss the mechanisms that can explain the appearance of this one-phonon density of states. As we mentioned in section 1, there are traditionally two models that try to explain experimental SERS results: the classical EM enhancement (long range) and charge transfer excitations, among other possible short-range mechanisms [15]. In contrast to the situation concerning the enhancement of the Raman spectrum of molecules by metallic particles or surfaces, where a lot of both experimental and theoretical work has been done, little information is found on lattice-phonon modes enhanced by the presence of metallic

particles in insulating crystalline matrices [5, 6]. So far, no theoretical model has been developed in detail for these systems.

In the dipolar limit of the classical model, and taking into account only the linear polarizability term (proportional to the electric field) [16], the Raman cross-section enhancement G_0 for an average molecule adsorbed on a spherical metallic particle of radius a and dielectric constant $\epsilon(\omega) = \epsilon_1(\omega) + i\epsilon_2(\omega)$ embedded in a medium of dielectric constant ϵ_0 is given by [17]

$$G_0 = |1 + 2g_0|^4 \tag{1}$$

with $g_0 = (\epsilon(\omega) - \epsilon_0)/(\epsilon(\omega) + 2\epsilon_0)$. Here ω stands for both incident- and dispersed-light frequencies, assuming small Raman shifts. The validity of this expression is limited to small spheres, say $a \leqslant \lambda_0/15$, where λ_0 is the laser wavelength, which is our case at least for samples S0–S3.

Substituting in (1) the optical constants of bulk Ca, Li and Ni metals at 2.23 eV (close to the maximum of the SP band for the three of them) and the refractive indexes of CaF_2 and MgO we estimate enhancement factors at the particle surface of 1.2×10^4, 3.8×10^5 and 1.5×10^2 for Ca(CaF_2), Li(MgO), and Ni(MgO) colloids, respectively. Although these numbers have to be taken as only an approximation they reflect the well known capability of alkali metals for SERS [2] as compared to transition metals, whose poor performance is related to strong plasma damping due to their high ϵ_2 values. Thus, though at 500 nm we are exciting just in the SP plasmon band of Ni colloids, the enhancement is expected to be orders of magnitude weaker than for Ca or Li particles, as observed.

(1) applies to an average over adsorbed molecules for a single colloid. In order to work out the total enhancement of a sample we must consider the spatial extension of the enhancement for each particle, integrate over the active region and multiply by the density of particles (N_p in table 1). Following the expression of [18], we assume a radial decay of the enhancement relative to the activity in the absence of the colloid as $(a/r)^{12}$, where r is the distance of the molecule from the colloid centre. If the activity of the molecule is independent of r the integration extends from a to infinity and a dependence of type $v_c N_p = V_c$ is obtained, where v_c stands for the volume of each particle and V_c for the total colloid fractional volume. This is apparently in agreement with the experimental result that the activated forbidden spectrum is roughly proportional to V_c. However, the following considerations must be made.

The classical EM enhancement arises from the enhancement of the electric field acting on the molecule. It is only dependent on optical constants of the metal and host medium, irrespective of the Raman-active molecule, and cannot (in the linear approximation) break parity- or momentum-conservation selection rules on its own, neither can it explain why some modes are more enhanced than others or why different compounds show such different enhancements in apparently the same conditions. Then, since we observe the whole density of CaF_2 and MgO phonons, there must be another mechanism activating the spectrum, though its resonant behaviour is undoubtedly due to SP excitation. The most probable one is the distortion of the lattice in the vicinity of the colloid, which, together with the discontinuity at the surface, result in loss of periodicity and breaking of the $k = 0$ selection rule. For small Ca colloids the compression induced by the colloid is absorbed coherently (without dislocations) by the host matrix in only a few layers. Therefore, in performing the integration to find the total enhancement, only a layer of a few ångstroms will contribute, since only in this layer is the whole density of phonons active. Then, the classical enhancement is expected to behave as a surface effect in our samples, and would be proportional to S_c (see table 1), contrary to observation.

Even if the dependence on V_c were valid, the density of colloids is so low that, although the enhancement for a single particle is very high, a relative increase of only about 10% (at best) is predicted for the whole sample.

Consequently, the EM mechanism, in its classical form, does not account for the totality of our experimental results, though it explains the resonant behaviour. A further step in the model, beyond the term linear in $\boldsymbol{E}$, is to consider the effect of the strong electric-field gradient at the colloid surface, which can break selection rules and activate forbidden modes. The gradient term has its own selection rules; it transforms as the hyper-Raman process [16] and can thus activate zone-centre infrared modes and change the activity of allowed Raman modes. However, it is difficult to justify how it could activate the whole density of $k \neq 0$ phonons. Moreover, since the electric-field gradient decays abruptly at 2 or 3 Å from the surface [16] its effect would be again proportional to the colloid surface and not to the volume.

These considerations do not mean that EM processes are not present, but indicate that we need the occurrence of other mechanisms providing the correct dependence along the samples studied and higher enhancement values.

We finally arrive at the charge-transfer (CT) model, which has been applied, in several forms, to explain short-range effects such as the 'first-layer' enhancement or the appearance of the one-phonon density of states and the continuum background in the Raman spectrum of alkali halides containing Ag colloids [5, 6]. As usually formulated, the CT model involves an electron–hole pair excitation from E_F to a 'CT state' from which the electron is transferred to the electroaffinity level of the adsorbed molecule [2]. Since the evidence of resonant enhancement upon excitation in the SP band is clear, we reformulate the model to emphasize the role of collective excitations in the following way.

(i) The incident photons, of energy $h\omega_L$ within the colloid band, excite surface plasmons in the metal particle. The occurrence of this process is proportional to the colloid volume.

(ii) Among several de-excitation paths, the electron sea can decay to excite an electron–hole pair, from which the electron can be transferred to the host if an energy matching occurs between the laser energy ω_L, the bottom of the host conduction band E_0 and the Fermi level of the metal E_F, such that $h\omega_L > E_0 - E_F$.

(iii) In the host, electron–phonon interaction takes place, as in usual Stokes or antiStokes processes, giving rise to single-phonon modes. The lattice distortion and loss of periodicity in the vicinity of the colloid break the $k = 0$ selection rule and account for the appearance of the whole density of states, and not only the allowed modes.

(iv) The electron is transferred back to the metal, where it recombines with the hole, re-emitting a photon, which is detected in the Raman experiment. The whole process appears as a resonance scattering of the host phonons when exciting in the SP band of the metal colloid.

In this process the transferred electron explores the host layers near the metallic surface, thus allowing for selection-rule breaking and providing the proportionality to the volume of the colloid, as observed.

One of the points in the model is the requirement that the laser energy ω_L be at least as great as $E_0 - E_F$. On varying ω_L one would expect an onset in the excitation curve of the activated spectrum intensity, below which the intensity should decay abruptly. We have unsuccessfully searched for such a cut-off in CaF_2 up to the limit of detector sensitivity. If it exists, it must be below 2 eV, as illustrated in figure 5.

A further step in the validation of the model is the behaviour predicted for different metals. Experimental results with other techniques support indirectly the CT mechanism

in these compounds: electron photoemission from metallic colloids following plasmon excitation is corroborated by two well known observations, photoconductivity [19] and photothermal bleaching of colloids [20]. In both experiments electrons are removed from the metallic precipitates by photon excitation in the colloid band. Although to our knowledge no photoconductivity experiments have been performed in CaF_2:Ca, not in MgO:Li, Ni, photothermal bleaching of Ca colloids in CaF_2 and of Li colloids in MgO can be achieved [20]. In contrast, photothermal bleaching of Ni colloids in MgO was unsuccessful [11]. This is presumably related to the larger work function of metallic Ni (4.5 eV in vacuum) as compared with Ca (2.8 eV) and Li (2.4 eV), thus placing the Fermi level of Ni colloids much deeper with respect to the MgO conduction band. Then $E_0 - E_F$ would be larger than the SP energy so that no CT would occur with the laser in the SP band. We note that, since the classical model also predicts a very low enhancement for Ni colloids, this argument is only a corroboration of the model but not an indisputable proof.

Finally, we would like to comment on the relative intensity of allowed-to-forbidden spectra. The fact that the allowed peak presents at the higher excitation energies an intensity comparable to that of pure CaF_2, and its partially resonant behaviour, can be interpreted in two ways.

(i) The peak arises from non-distorted areas of the sample. Those far from the colloid give the non-resonant contribution, as in pure CaF_2, while those close to the colloids, where SERS occurs but periodicity is conserved, so that forbidden spectrum is not activated, account for its resonant behaviour.

(ii) The resonant part arises from the distorted region surrounding colloids, such as any other phonon of the density of states, and is activated through the SP+CT mechanism described above. The mode keeps a 'memory' of its allowed character and is therefore higher and narrower than the others. The question in this case is: why is the relative intensity not the same in all samples? In S3 or S4, where the amount of colloid mass is greater, the activated phonon spectrum is much more intense than in S1 or S2. The allowed mode should be proportionally enhanced if case (ii) holds. Since this is not observed we suggest that the resonant behaviour of the allowed mode is due to classical EM enhancement in non-distorted regions of CaF_2. The increasing volume fraction of regions perturbed by the colloids versus undistorted areas explains the increasing ratio of activated spectrum (mostly CT process) to allowed mode (mostly classical model) on going from S1 to S4.

5. Conclusions

We have reported SERS of CaF_2 and MgO phonons by small Ca and Li particles, respectively. The Raman spectrum corresponds to the one-phonon density of states of the host and does not depend on the particle size in the 3.5–25 nm region. Its intensity depends linearly on the metal volume fraction. Contrary to other observations the spectrum is partially polarized, showing in CaF_2 a partial T_{2g} character. After discussing the validity of classical EM models, we suggest that the activation and resonant enhancement of the one-phonon density of states can be explained by a mechanism involving plasmon excitation followed by electron transfer to the matrix, whereas the resonant behaviour of the allowed mode can be of purely EM origin.

Acknowledgments

We are grateful to Dr J M Calleja, from the Universidad Autónoma de Madrid, Spain, for his availability and help in performing measurements with dye-laser excitation. P B Oliete thanks DGA for financial support.

References

[1] Fleischmann M, Hendra P J and McQuillan A J 1974 *Chem. Phys. Lett.* **26** 13
[2] Otto A, Mrozek I, Grabhorn H and Akemann W 1992 *J. Phys.: Condens. Matter* 4 1143
[3] Otto A 1984 *Light Scattering in Solids* vol IV, ed M Cardona and G Guntherodt (Berlin: Springer) ch 6
[4] Rzepka E, Lefrant S and Taurel L 1979 *Solid State Commun.* 30 801
[5] Abel H-B and Fischer F 1987 *Phys. Status Solidi* b **144** 875
[6] Abel H-B and Fischer F 1991 *Phys. Status Solidi* b **167** 741
[7] Orera V M and Acalá R 1976 *Phys. Status Solidi* a **38** 621
[8] Orera V M and Acalá R 1977 *Phys. Status Solidi* a **44** 717
[9] Hobbs L W 1976 *J. Physique Coll.* C7 **37** 7
[10] Narayan J, Chen Y and Moon R M 1981 *Phys. Rev. Lett.* **46** 1491
[11] Chen Y and Orera V M 1986 unpublished results
[12] Sangster M J L, Peckham G and Saunderson D H 1970 *J. Phys. C: Solid State Phys.* 3 1026
[13] Elcombe M M and Pryor A W 1970 *J. Phys. C: Solid State Phys.* 3 492
[14] Shuker R and Gammon R W 1970 *Phys. Rev. Lett.* **25** 222
[15] Burstein E, Chen Y J, Chen C Y, Lundquist S and Tosatti E 1979 *Solid State Commun.* **29** 567
[16] Sass J K, Neff H, Moskovits M and Holloway S 1981 *J. Phys. Chem.* **85** 621
[17] Kerker M, Wang D-S and Chew H 1980 *Appl. Opt.* **19** 4159
[18] McCall S L, Platzman P M and Wolff P A 1980 *Phys. Lett.* 77A 381
[19] Jain S C and Arora N D 1974 *J. Phys. Soc. Japan* **36** 739
[20] Orera V M and Alcalá R 1976 *Solid State Commun.* **27** 1109